fMRI Scanning Methods

20

Chris J. Conklin and Devon M. Middleton

Introduction

Over the past three decades, a tremendous amount of research and development have been dedicated to enhancing the diagnostic capabilities of magnetic resonance imaging (MRI) within clinical medicine and neurosciences. As new techniques emerge, the complex mechanisms governing processes such as cognition, emotional response, and behavioral tendencies are becoming disentangled from one another, thus opening possibilities for imaging biomarker development and validation of indication-specific pathophysiologic models. Higher field strengths, high-performance imaging gradients, more densely packed multichannel signal receiver electronics, and innovative pulse sequence designs are enabling more granularity to isolate and quantify dynamic physiologic cascades with the ultimate hope of clinical standard-of-care integration. This chapter will focus on a high-level description of the physics, methods, and advancements in the functional MRI (fMRI) domain with a particular emphasis on blood oxygenation level dependent (BOLD) imaging.

Simply stated, BOLD fMRI relies on the detection of changes in MR signal as a result of local susceptibility changes in hemoglobin oxygenation response to neuronal activity. All brain activity is a chemical reaction, with synaptic firings precipitating an increased energy demand that is typically met through oxidative glucose metabolism. When a specific brain region experiences activity, arterioles in proximity dilate, leading to an increase in blood flow in downstream capillaries surrounding active neurons. Subsequently, the amount of local oxygen as a result of brain activity surpasses the satisfaction requirements to meet metabolic need. This abundance of oxygen binds with the ferrous iron in the heme molecule to create diamagnetic oxyhemoglobin, thereby reducing susceptibility (relative to the paramagnetic deoxyhemoglobin) and increasing MRI signal. By deploying a sequence sensitive to susceptibility effects, such as T2* contrast, signal differences between imposed active and "resting" conditions can be observed and analyzed to correlate with gray matter structures involved with task completion. Further details regarding the physics behind the most common pulse sequences as well as advances in fMRI will be detailed in the coming sections.

Magnetic Resonance Physics

MRI is the diagnostic tool of choice for anatomical imaging as it offers exceptional soft tissue contrast with high in-plane resolution. Generating relevant MR signals requires manipulation of the hydrogen atoms within the human body, which is the ideal choice given that the human body by weight is roughly two-thirds water. The hydrogen atom also has some convenient quantum properties such as the presence of a single magnetic moment and two unique spin states, further solidifying it as the ideal target for MRI. When placed in a large, static magnetic field ($\boldsymbol{B}_0$) the nucleus (proton) of the hydrogen atom mimics the behavior of a compass needle as it becomes magnetized. The application of an external static magnetic field $\boldsymbol{B}_0$ to a single nucleus, which will be referred to as a *spin*, or an aggregate of spins, induces an angular momentum forcing a rotation about the axis of its magnetic moment. This phenomenon is called *precession* and is one of the most fundamental principles of MRI. Spins can align themselves in one of two states relative to the $\boldsymbol{B}_0$: parallel and anti-parallel. Parallel spins reside in a lower energy states, while those anti-parallel occupy a higher energy state, which is depicted in Fig. 20.1. Even in the presence of an external magnetic field, the distribution of parallel and anti-parallel spins remains completely random, but a small yet significant number of unpaired nuclei exists and is aligned with $\boldsymbol{B}_0$. The sum of those magnetic moments aligned with the static field

C. J. Conklin (✉)
Neuroscience Medical Affairs, Bioclinica, Princeton, NJ, USA

D. M. Middleton
Department of Radiology, Thomas Jefferson University, Philadelphia, PA, USA
e-mail: Devon.Middleton@jefferson.edu

S. H. Faro, F. B. Mohamed (eds.), *Functional Neuroradiology*, https://doi.org/10.1007/978-3-031-10909-6_20

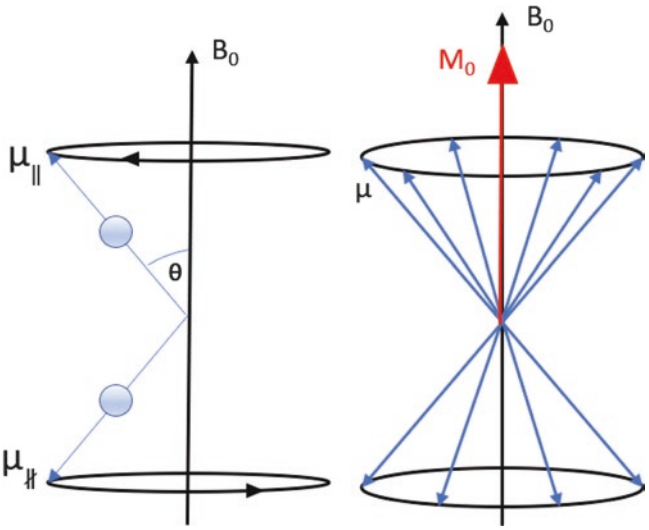

Fig. 20.1 *Left*: Spins in the presence of an external magnetic field $\boldsymbol{B_0}$ can occupy one of two spins states, spin up (parallel) or spin down (antiparallel) and precess about the field at the Larmor frequency. *Right*: There is an excess of spins aligned with $\boldsymbol{B_0}$ that form a net magnetization vector, $\boldsymbol{M_0}$

yields a net magnetization vector ($\boldsymbol{M}_0$). The management of the electromagnetic forces $\boldsymbol{M}_0$ experiences and the measurement of its response to them are the key element behind MR signal generation.

The excitation of $\boldsymbol{M}_0$ generates the stimulated echo, or signal, that captures the tissue-specific information local to a targeted region of interest. The unpaired nuclei that constitute the net magnetization vector are capable of absorbing electromagnetic quanta in the radiofrequency (RF) spectrum. Absorption requires matching the frequency of spin precession with the frequency of the RF field. This frequency is called the *Larmor frequency*, which is a linear function of hydrogen's gyromagnetic ratio and the static field strength of $\boldsymbol{B}_0$. Once this resonance condition is satisfied, the unpaired nuclei undergo a series of energy transitions via the absorption and emission of electromagnetic quanta. At equilibrium, insufficient energy exists within the system to precipitate energy level transitions. By introducing transient, time-varying magnetic fields that meet the resonance condition, the frequency of the oscillating magnetic field, called a *radio frequency pulse*, matches the precessional frequency of the spins (i.e., Larmor frequency).

Macroscopically, the aggregation of parallel spins constitutes the net magnetization $\boldsymbol{M}_0$, which is then subjected to a selective RF pulse. These spins absorb photons and transition to a higher energy state and become *excited*. The RF pulse that elicits this response is known as an *excitation pulse*. A favorable consequence of this RF excitation is that transitioning to a higher energy state causes the group of unpaired spins to become *tilted* such that their spin state is no longer parallel with the $\boldsymbol{B}_0$ field. As the number of hydrogen nuclei absorbing quanta increases, $\boldsymbol{M}_0$ continues to deviate further from the parallel state creating a larger degree of deflection relative to $\boldsymbol{B}_0$. This degree of deflection is called the *flip angle, α,* and is a measure of the amount of spins located in the higher energy state. The amplitude, frequency, and duration of the RF excitation pulse ultimately dictate this quantity. Simply stated, the interaction of an excitation pulse with the net magnetization vector leads to a tipping of $\boldsymbol{M}_0$, subsequently spawning a transverse magnetization component central to MR signal generation.

The application of transient RF excitation pulses allows tracking and characterization of the dynamic changes experienced by $\boldsymbol{M}_0$. As described above, when a pulse is emitted, the magnetization vector tips away from the longitudinally aligned $\boldsymbol{B}_0$ field. Once the applied RF pulse ends, two independent processes work to restore equilibrium. The newly formed transverse magnetization vector, $\boldsymbol{M}_{xy}$, decays as a result of spin–spin interactions. Since each spin can be viewed as a single magnetic moment, perturbations between neighboring nuclei manifest as magnetic field inhomogeneities. These inhomogeneities create local field gradients that change the precessional frequency of spatially dependent nuclei (as the Larmor frequency is a function of the field strength). This altering of precessional frequencies induces a loss in coherence between the nuclei that make up the net magnetization, a process known as *dephasing*, which gradually reduces the transverse component of the net magnetization vector. Consequently, as the phase of individual spins uniformly distributes and erodes the transverse magnetization, the longitudinal magnetization, $\boldsymbol{M}_z$ (aligned with $\boldsymbol{B}_0$), systematically increases in magnitude to reestablish equilibrium (see Fig. 20.2).

The mechanism with which spins return to this lower energy state is called spin-lattice regrowth, the resulting effect from nuclei interacting with their local microenvironment. The combination of the T2 (spin-spin) and T1 (spin-lattice) relaxation phenomena makes possible the creation and measurement of meaningful, tissue-specific, MR signal within the regional excitation plane. Simply stated, signal generation is the result of an induced current arising from the net magnetic moment, the aggregate of coherent (in-phase) spins, and precessing about the longitudinal axis of the static $\boldsymbol{B}_0$. The precession of spins is precipitated through the application of an RF excitation pulse having a carrier frequency at or near the Larmor condition for the hydrogen atom. This pulse tips $\boldsymbol{M}_0$ into the transverse plane (i.e., no longer parallel to $\boldsymbol{B}_0$), with stronger RF pulses yielding greater deflection, and allows for the relaxation processes to occur. The rate at which the transverse magnetization decays and the longitudinal magnetization grows is a function of the local microenvironment, subsequently providing image contrast between differing biological tissues.

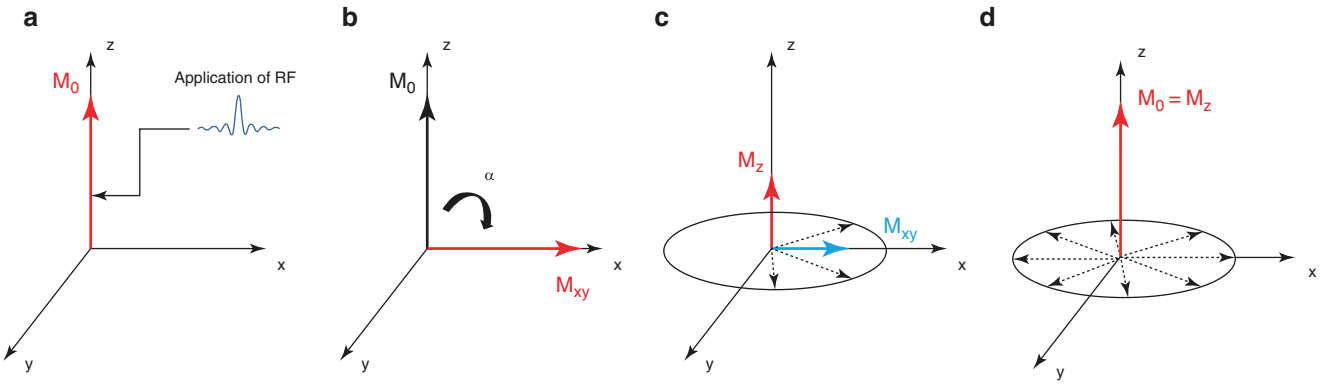

Fig. 20.2 Illustration of excitation process and relaxation rate evolution. Initially, the net magnetization vector $\boldsymbol{M}_0$ is aligned along the *z*-axis with the static field $\boldsymbol{B}_0$ (**a**). After application of the RF excitation pulse, $\boldsymbol{M}_0$ is tilted into the transverse, *xy*, plane (**b**). As spin-spin interactions occur the transverse magnetization $\boldsymbol{M}_{xy}$ diminishes due as phase coherence is lost (**c**), ultimately regrowing along the *z*-axis to return to equilibrium (**d**). Please note that $\boldsymbol{M}_0 = \boldsymbol{M}_z + \boldsymbol{M}_{xy}$

The next critical component to focus on is receiving and reconstruction of the induced signal. As described above, magnetic field inhomogeneities create phase incoherence, the duration of which dictates the T2 relaxation constant for a given tissue type. However, these field inhomogeneities also provide spatial information, which is essential for MR signal localization. By introducing well-defined and precise magnetic field inhomogeneities, spin coherence can be manipulated in a predictable manner. Since the precessional frequency of spins is related to the magnetic field strength, application of additional, linearly varying fields can alter the rate of precession based on spin location. These alternating magnetic fields arise through the use of *gradient coils*, which are large coils positioned along the three orthogonal axes (i.e., *x*, *y*, and *z* dimensions). When current is passed through these coils, it generates a magnetic field thereby allowing for the spatial distribution of precessional frequencies and phases local to a given magnetized sample. This enables the frequency content of the MR signal to be analyzed, also called *frequency encoding*. This is used to fill in one axis of *k*-space, which is the frequency analog of spatial domain signals. These signals are not aligned in the traditional Cartesian *x*–*y* axes, rather, signal data is collected and sampled by frequency and phase encoding axes in *k*-space. Continuing to apply field gradients at specific time points during acquisition allows for the construction of an MR signal "grid," each with its own unique phase, frequency, and spatial coordinate, called spatial encoding [1]. Conversion of *k*-space information back to the spatial domain requires the use of a Fourier transform. The process is called *reconstruction* and is necessary to allow clinicians and researchers the ability to visualize and probe, both qualitatively and quantitatively, the inherent water characteristics of the imaged volume. Direct extension of these principles enables the ability to image, track, and investigate oxygen content within blood during heightened brain activation.

Acquisition Schemes

The mechanism through which the net magnetization vector ($\boldsymbol{M}_0$) is manipulated and gradient coils are choreographed to spatially encode the MR signal varies and is typically a function of indication as well as application. The ordering and synchrony of RF pulses and gradient play outs used to excite spins and acquire MR signal is called a *pulse sequence*. They can vary greatly, and each has its own characteristics that can be manipulated to modulate signal intensity from excited spins contained within specific tissues of interest. MRI is a field of tradeoffs and balancing signal-to-noise ratio (SNR), resolution, and acquisition time with the desired contrast is central to protocol design. The following section will detail the key pulse sequences commonly used in fMRI protocols to help drive the decision on choosing an optimal approach.

Spin Echo

Spin-echo (SE) sequences require the use of two distinct types of RF pulses: excitation and refocusing as initially observed and discovered by Erwin Hahn [2]. Excitation pulses tilt the bulk longitudinal magnetization vector, aligned with $\boldsymbol{B}_0$ at equilibrium, into the transverse plane. Once the imaged sample is no longer exposed to the RF pulse nor additional gradient fields, spins begin to dephase relative to one another (T2 decay) leading to a net reduction in the transverse magnetization component and a loss in overall MR signal as the system returns to a lower energy state. This

disappearance of coherence is a natural phenomenon and is referred to as *free induction decay* (FID). While relevant information about tissue microstructure can be extracted from the FID signal, SE sequences rely on regaining phase coherence through the application of another RF pulse to form a signal echo. An echo contains a more comprehensive characterization of the imaged microenvironment compared to a FID as it allows precessing spins to experience both T1 and T2 relaxation mechanisms, both of which provide the basis for the superior soft tissue contrast inherent to MRI acquisitions. Additionally, the timing of the echo formation as determined by pulse sequence parameters allows for manipulation of contrast between spins with differing relaxation constants. A classic spin echo sequence is characterized by a 90° excitation pulse, to perturb the net magnetization vector and project it into the transverse plan, followed by a 180° refocusing pulse to reverse the natural dephasing process spins experience and create a signal echo. It is important to note that in a static environment, the refocusing pulse will perfectly restore any accumulated phase and provide maximal MR signal. This can be conceptualized in Fig. 20.3. Imagine two runners, one wearing red and the other green. Both runners start at the same position (analogous to immediately after the excitation pulse) and the red runner is traveling faster than his or her opponent. Assume now that at some point the runners are forced to swap lanes (due to the refocusing pulse) and continue at their current speed. Barring any other changes, they will arrive at the same location at some measurable amount of time, which is when the race will finish and the echo generated. However, in practice, water molecules randomly diffuse and can have an impact on the collected MR signal as a function of the distance traveled relative to the spatial extent of inhomogeneity. This will be discussed in further detail below.

The playout of the refocusing pulse in a spin-echo sequence occurs at a well-defined instance, typically $T_E/2$, where T_E represents the time it takes for the newly coherent spins to generate an echo. This is called the *echo time*. The echo signal is encoded in a frequency and phase location in *k*-space dictated by spatially selective gradients that will be subsequently transformed into image space during reconstruction. Figure 20.4 depicts a basic spin-echo pulse sequence diagram. Spatial selectivity is achieved through the deployment of three independent and orthogonal gradients: the slice select(ion) gradient, G_{SS} (in red), the frequency encode gradient, G_{FE} (in blue), and the phase encode gradient, G_{PE} (in green). A section, or slab, of water molecules can be targeted through the application of the slice select gradi-

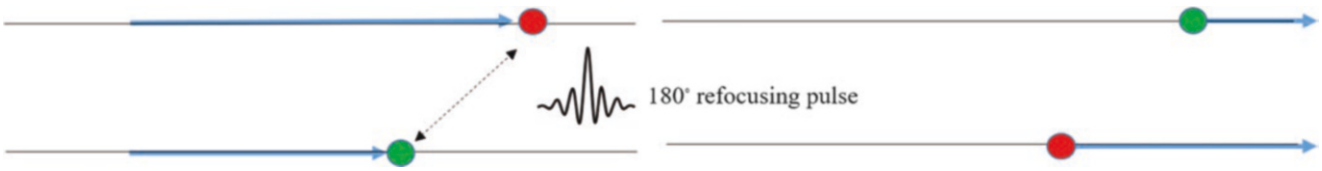

Fig. 20.3 A representation of what spins experience after the spin-echo refocusing pulse. The pulse is analogous to two runners swapping lanes such that they arrive at the "finish line" in unison, thereby creating an echo

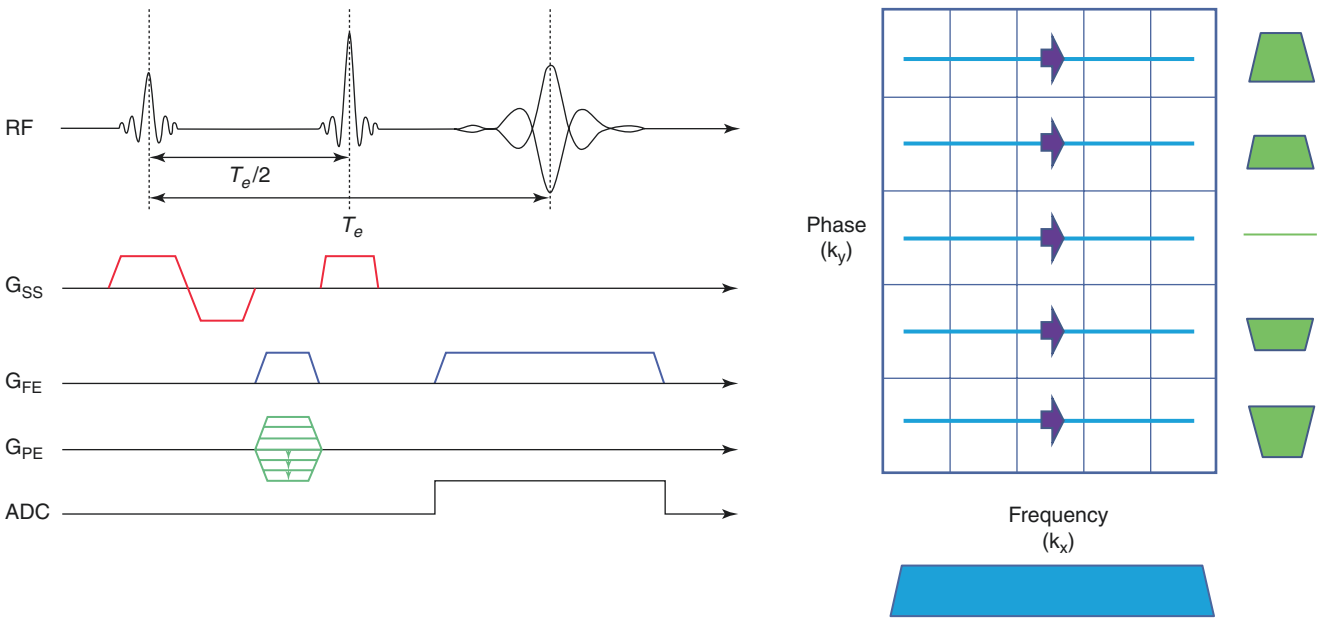

Fig. 20.4 Standard spin-echo pulse sequence diagram and associated *k*-space traversal

ent, which linearly varies the magnetic field through the slice plane. By delivering the excitation pulse concurrently with the gradient, the range of frequencies contained within the RF profile (the bandwidth) can be translated to the desired range of spatial locations within the imaging plane. A fixed bandwidth the thickness of the excited slice can be altered by varying the amplitude of G_{ss}. Immediately following this process, a slice rephasing gradient (the lobe of opposite polarity along the slice select direction) is turned on to correct for any phase dispersion as a result of slice selection. Without this, signal loss would occur since the slice select gradient acts like a spoiler past the isodelay point.

Once the net magnetization within the location of interest has been excited and tipped into the transverse plane, additional localization is required to resolve the origin of the signal in a voxel-wise sense. As noted above, this can be achieved by pulsing two additional gradients, G_{FE} and G_{PE}, along the other two axes, orthogonal to the slice selection direction, in a process known as spatial encoding. The frequency encoding gradient assigns a unique precessional frequency to each spin group along the gradient, each with its own distinct location. Frequency encoding is typically a two-step process, needing both a prephasing component (prior to the refocusing pulse) in addition to the final gradient readout lobe (after refocusing). The prephasing gradient introduces an initial phase dispersion necessary for echo generation. Once this phase dispersion is reversed by the refocusing pulse, the readout gradient is played to continue phase accumulation until an echo is created. Similarly, phase encoding occurs in the last independent gradient direction and tends to occur during the prephasing stage. The degree of phase variation is determined by the area of the phase encode gradient, thereby prescribing a discrete phase during spin precession that reflects spatial location. This necessitates modifying the phase encode gradient amplitude each repetition time (TR) until full coverage of the imaging region is achieved.

Gradient Echo

The simplest and most basic of pulse sequences is the *gradient echo* (GRE), once again initially observed by Hahn [3]. MRI contrast is a function of both the T1 and T2 relaxation rates; however, GRE contrast is also dependent and sensitive to magnetic field inhomogeneities. This additional dependence is called the T2* contrast and is central to probing signal changes due to the presence of paramagnetic ions and/or molecules. The utility of GRE acquisitions is the rapid manner in which images can be acquired, even in three dimensions (3D), making it an attractive candidate for vascular imaging, including *blood oxygenation level dependent* (BOLD) imaging, which is ubiquitous now for fMRI [4]. Gradient echo techniques are also called gradient-refocused echoes, gradient-recalled echoes, or field echoes. The term field echo is used as it describes the magnetic field formed by the frequency encode gradient that rephases the GRE to produce a meaningful MR signal. The hallmark of GRE sequences is that only a single RF pulse, the excitation, is required to precipitate the cascade of physical interactions needed to generate the received signal, or echo, and no refocusing RF pulse is used. Rather, a series of gradient reversals along the frequency encode axis allows for a return to phase coherence leading to the creation of the desired echo. This is in contradistinction to the refocusing RF pulse required for spin-echo formation that restores phase coherence and the subsequent transverse magnetization used for MR signal detection. GRE sequences initially deploy a prephasing gradient lobe to induce phase incoherence of the spin isochromats, which are groups of similarly behaving spins. As noted above, the presence of this gradient field increases the rate of spin dephasing due to alteration of the precessional frequencies as a result of additive magnetic field effects. Spins exposed to stronger fields have larger frequencies than those in weaker fields. This accelerated loss of phase coherence persists until the external gradient is turned off, typically at the point when the bulk transverse magnetization has been almost destroyed, and is left deactivated to avoid further gradient induced decay. Immediately pulsing a gradient lobe of opposite polarity reverses this effect, forming a maximal echo when the area of both gradient lobes is equal in magnitude (see Fig. 20.5, blue shaded regions).

The application of a reversed gradient field forces the spins that experienced a higher precessional frequency to slow down and assume the rate of precession of those spins that were trailing during the initial application of the dephasing lobe (those in the weaker field). Similarly, those spins that were lagging are now chasing the previously faster moving spins (see Fig. 20.6). Spin 1 (a) is dephasing more rapidly than spin 2 (b) during the gradient dephasing period. Once the prephasing gradient is turned off and a new gradient is applied with equal, but opposite, polarity (the readout gradient), the spins begin to gain coherence until an echo is formed. Another perspective is shown in Fig. 20.7.

Assume that our red/green runners are performing a 100 m dash. At the start of the race, the prephasing phase, the red runner is traveling much faster than his opponent. These runners continue to maintain their pace for that entire initial phase until they are instructed to immediately stop, turn around, and race back to the starting line (the readout phase). Each runner still maintains his or her same initial rate of travel and subsequently both finish at the same time. This is analogous to regaining transverse phase coherence and is what leads to the formation of a gradient echo. The time it takes for the spins to rephase and regain transverse phase coherence is identical to the time it took to dephase them, assuming no energy losses as a result of spin–spin interactions.

The lack of a refocusing pulse in gradient echo formation reduces overall RF power emitted by the transmit coil and

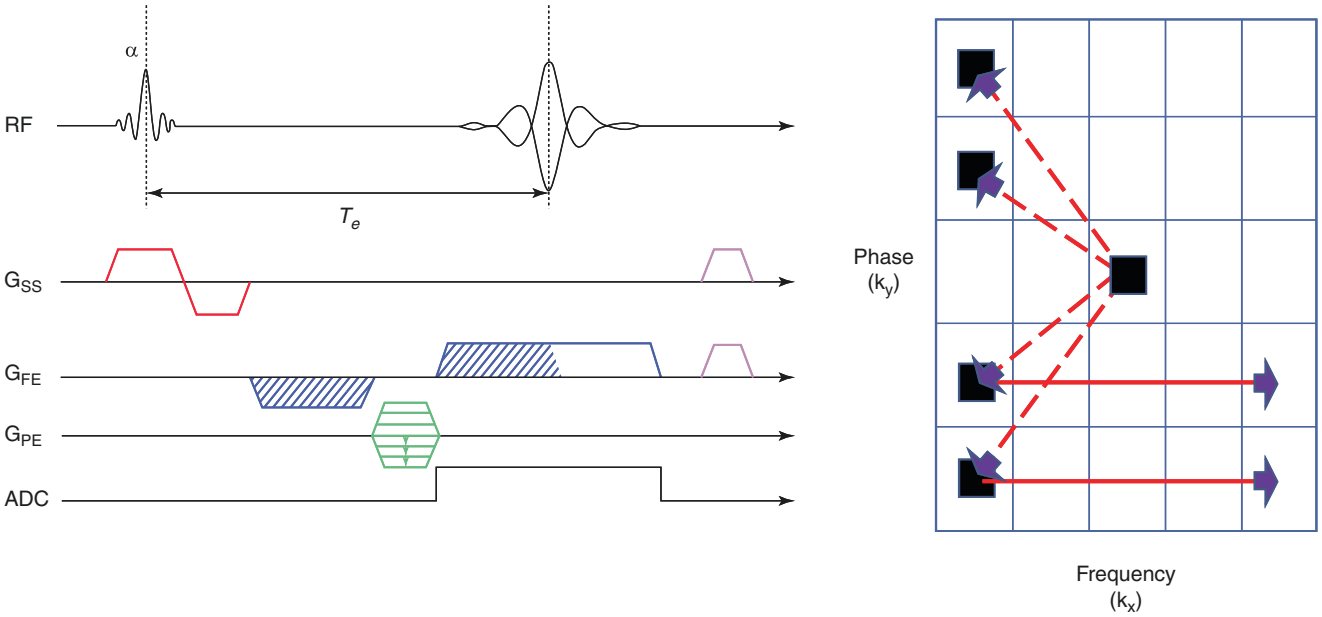

Fig. 20.5 Standard gradient echo pulse sequence diagram with *k*-space traversal

Fig. 20.6 Illustration of echo formation in a GRE sequence. Prior to prephasing, spins are losing phase coherence (*left*). Once a readout gradient is deployed coherent is gained (*center*) until an echo is formed (*right*)

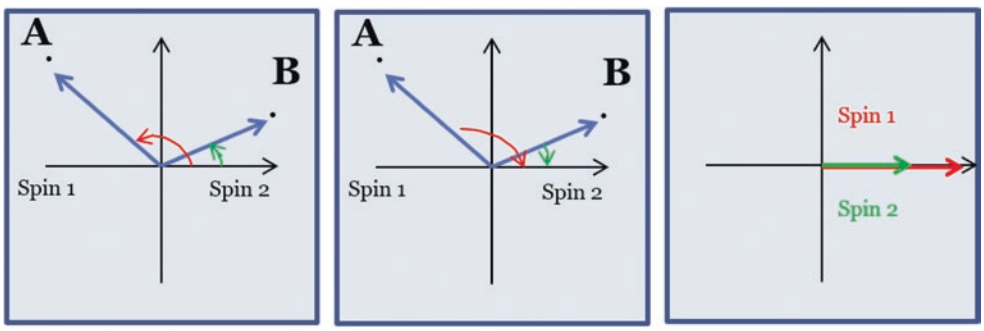

Fig. 20.7 Gradient echo formation diagram. Two spins are dephasing at different rates prior to rephasing readout. The gradient playout is analogous to two runners turning and running back to the "start line" to create an echo

thus the amount of energy absorbed by tissues influenced by the field, making it a safer sequence for clinical use and enabling a faster acquisition because RF pulses can be more densely packed without exceeding specific absorption rate thresholds. This is particularly true at higher strength scanners where more RF energy is required to "excite" the larger net magnetization vector. Despite this advantage, the absence of the refocusing pulse increases the sequence's sensitivity to the presence of magnetic field inhomogeneities by failing to null any residual phase accumulation as a result of dephasing spins as in spin echo sequences. GRE sequences are therefore more prone to image contamination from field inhomogeneities and susceptibility effects, as any amount of phase accumulation due to local inhomogeneity introduced by factors outside of the gradient fields are uncompensated during echo formation and thus degrade overall MR signal.

GRE sequences typically have shorter scan times than SE sequences, in part due to the lack of a refocusing pulse, but

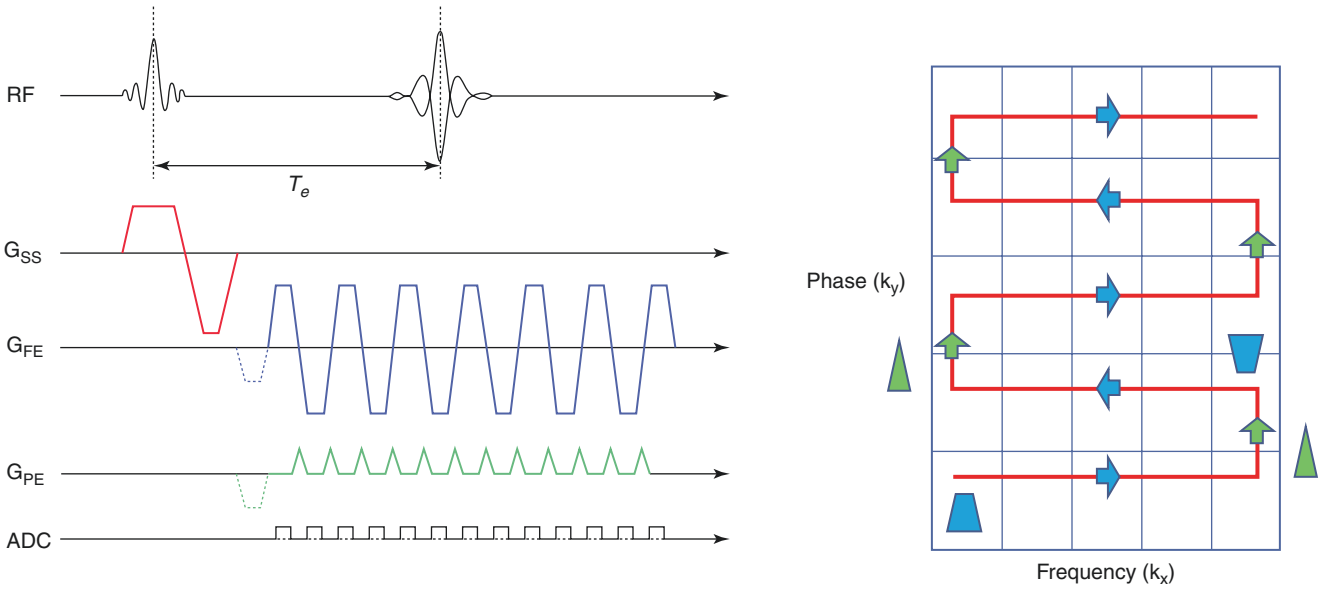

Fig. 20.8 Typical GRE-EPI pulse sequence diagram. The green phase encode gradient is "blipped," which allows for the zig-zagged *k*-space traversal seen on the right

also because a pure 90° magnetization tilt into the transverse plane is not needed. As noted earlier, spin coherence in GRE sequences is obtained through the nullification of spin-phase changes with gradient reversals. The amount of phase angle induced is a function of the amplitude-time product. Stronger gradients can achieve the desired phase angle in a shorter amount of time resulting in a substantially reduced TR. However, manipulating the gradients in this fashion gives the transverse magnetization signal component insufficient time to decay fully after the signal collection period and prior to the application of the next TR's excitation pulse. This residual magnetization can persist throughout subsequent excitations, receive compounded imprinting from repeated relaxations and phase accumulations, and impart undesirable signal characteristics within the acquired MR data. One common approach to mitigate image contamination as a result of lingering transverse magnetization is to deploy "spoiler" gradients, which effectively destroy the remaining bulk transverse components, prior to the next excitation block. Spoilers can also be played out concurrently on multiple axes to reduce overall imaging time prior to the start of the next excitation pulse (see Fig. 20.5, purple trapezoids).

Echo Planar Imaging

Echo planar imaging (EPI) is an acquisition scheme characterized by an extraordinarily high sampling rate. Initially developed by Peter Mansfield, this sequence is capable of acquiring an entire brain volume with a single excitation pulse through an elegantly orchestrated spatial encoding process [5]. An EPI sequence diagram is shown in Fig. 20.8. Notice the high degree of similarity with the GRE sequence in terms of RF and slice select gradient playout, with the difference residing in the manner with which the frequency and phase encode gradients behave.

This type of EPI sequence is called a GRE-EPI. Similar modification can be made to the spin echo sequence (as is done for diffusion sensitized acquisitions) because EPI is strictly a readout strategy used for fast imaging applications that requires high-performance gradients for rapid on-off switching. Despite the generic GRE sequence being classified as a rapid acquisition, it still needs multiple excitations to sample the entirety of the imaging volume resulting in a temporal resolution incapable of capturing subtle, transient physiologic changes induced by neural stimulation necessary for observing the BOLD effect. EPI alleviates this limitation by increasing temporal resolution through a rapid traversal of *k*-space while remaining sensitive to BOLD imprints left on the MR signal in a technique known as single-shot (SS) EPI. To date, most clinical BOLD applications are used for brain pre-surgical motor and language mapping and employ the SS-EPI sequence. Multishot (MS) variants exist, where *k*-space filling is broken into segments, which are less demanding on the gradients system and provide fewer phase error accumulations. However, MS-EPI acquisitions are longer and more susceptible to motion related artifacts.

SS-EPI sequences acquire signal through a series of gradient reversals. Each gradient echo can be uniquely encoded in-plane enabling *k*-space to be sampled under a single FID

envelope. Rapid oscillations along the frequency encode direction create an echo train where the polarity of the gradient lobe dictates the direction of *k*-space traversal. Simultaneous pulsing of the phase encode gradient, called blips, advances the *k*-space line in the phase encode direction. This is depicted in Fig. 20.8 (green line). The initial concurrent playout of both phase and frequency gradients initializes the first sample point in *k*-space (in this case the lower left point). A positive gradient in the frequency direction fills the first read-out line from left to right. Blipping the phase encode gradient while delivering a negative frequency encode lobe bumps collection to the next phase line and advances the readout from right to left. This zig-zag type scheme is repeated until the entire imaging volume is sampled. It is important to note that while an echo is generated for each gradient lobe, only the central echo (where the net encoding in both phase and frequency direction is zero) is used to determine the echo time, which is the point of maximal signal, and controls the image contrast.

BOLD imaging relies on the presence (or absence) of paramagnetic deoxygenated blood in a given region of interest. As noted earlier, GRE-based sequences are sensitive to field inhomogeneities due to their T2* contrast.

Applications

BOLD

The rapid nature of the SS-EPI sequence is ideally suited for interrogating and capturing subtle changes in the brain elicited by neuronal activity. Blood oxygen level dependent (BOLD) imaging is an imaging technique sensitive to transient MR signal changes caused by the differing magnetic properties exhibited by oxyhemoglobin and deoxyhemoglobin (dHb) [6, 7]. Deoxyhemoglobin is a paramagnetic substance that will interact with the applied magnetic field, $\boldsymbol{B}_0$, and create localized inhomogeneities within the imaging volume. These inhomogeneities lead to rapid spin dephasing and an overall decrease in MR signal. As brain activity increases, oxygen consumption increases in response to elevated metabolic demand. After an initial local decrease in oxyhemoglobin, vessels in the active region dilate resulting in an inrush of oxygenated blood. This phenomenon is referred to as the hemodynamic response and is central to BOLD imaging. This inrush results in a higher-than-baseline oxyhemoglobin concentration, reducing local magnetic susceptibility and driving a higher T2* signal. The physiological basis of BOLD is shown in Fig. 20.9.

Optimization of BOLD MRI

As with all MRI, EPI BOLD scanning methods need to be optimized to maximize clinically relevant signals while mitigating sources of contamination. This is of particular importance in the pre-surgical motor and language mapping applications where derived BOLD maps are used for tumor resection planning as well as intraoperative guidance. Choice of TR, TE, or the number of dynamics/measurements acquired all have an impact of the quality of the data. For example, when using a GRE-EPI based sequence, BOLD contrast is maximized when TE ≈ T2* of gray matter. However, the longer the TE, the more prone the BOLD acquisition becomes to susceptibility-induced signal dropout and a concomitant decrease in SNR. Similar issues arise

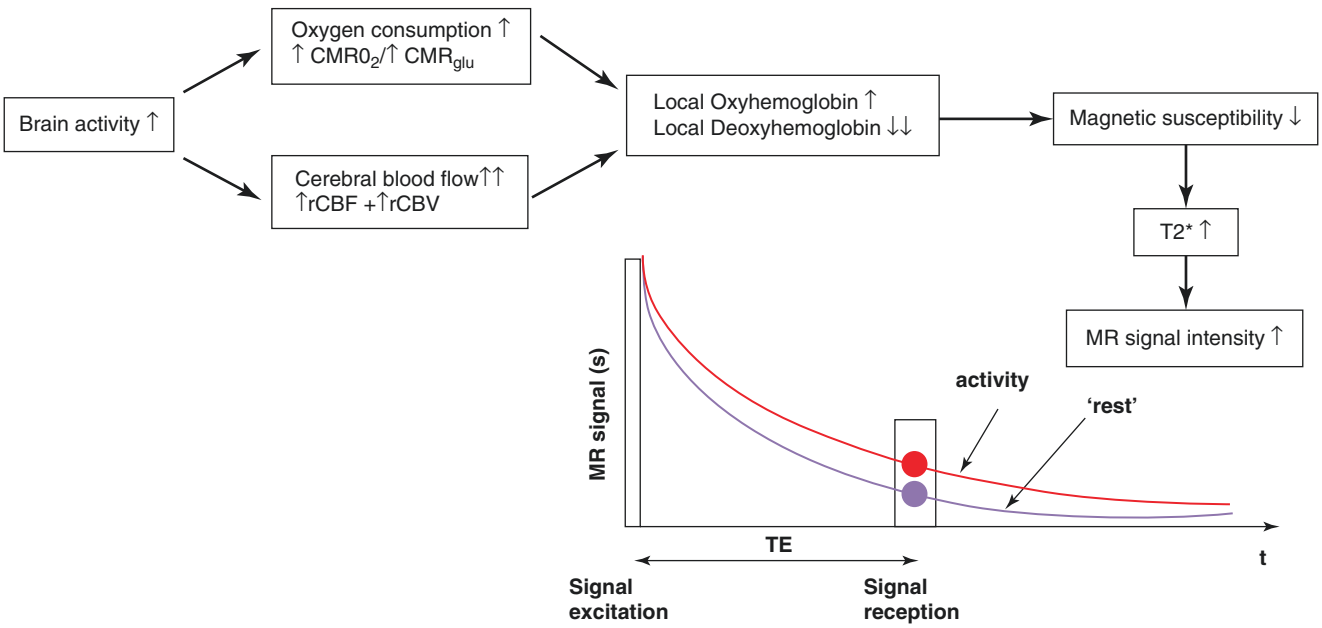

Fig. 20.9 Neurophysiologic basis of BOLD signal. MRI signal during active blocks is higher relative to "rest"

Table 20.1 Recommended BOLD imaging parameters from the Quantitative Imaging Biomarker Alliance (QIBA)

Imaging parameter	Recommended setting
Field strength	1.5T or 3T
Sequence type	GRE-EPI
Field of view (FOV)	240 mm
Slice thickness	3–5 mm
Number of slices	20–36
Repetition time (TR)	1.5–3 s
Echo time (TE)	30–35 ms at 3T; 40–50 ms at 1.5T
Measurements	90–256
Flip angle	90
NEX	1
Parallel imaging	Not used

from choice of TR value. A shorter TR enables a more comprehensive characterization of the hemodynamic response function through increased temporal resolution and thus more activation-related confidence but could introduce inflow effects from unsaturated spins. These unsaturated spins contribute to the entirety of their magnetization to the system, making it difficult to determine whether the increase in signal is due to perfusion or oxygenation, which could potentially confound image interpretation and increase false-positive activation. Partial volume averaging through slice thickness selection, geometric distortions as a result of echo train length, and cross talk as a result of slice acquisition ordering are also important pitfalls to avoid. Table 20.1 provides a parameter summary from the fMRI Radiological Society of North America (RSNA) Quantitative Imaging Biomarker Alliance (QIBA) committee (https://www.rsna.org/en/research/quantitative-imaging-biomarkers-alliance), an organization that strives to standardize the acquisition and analysis of BOLD images to transition the technique more firmly into the clinical domain [8]. Below is an example of optimized parameters for sensorimotor mapping.

Beyond imaging parameters, an additional consideration for the optimal acquisition of BOLD images relates to the plane of imaging. A common convention is to align the slice prescription angulation parallel to the anterior commissure—posterior commissure line. This convention has been kept for historical reasons where early registration and normalization procedures needed an anatomical landmark to provide accurate results. Depending on the brain regions of interest, if an area resides in a high susceptibility location, the slice plane can be angled tangentially to the inferior portion of the frontal lobe and the inferior portion of the cerebellum. By tilting the acquisition so drastically, the excitation and slice profiles will avoid the maxillary sinuses and help mitigate signal dropout due to susceptibility.

Z-Shim EPI

While GRE-EPI sequences excel at sampling the hemodynamic response with sufficient temporal resolution to calculate task-based correlations with observed MRI signal, sensitivity to field inhomogeneities has the potential to limit the accuracy of results in high susceptibility regions such as the orbito-frontal cortex, inferior temporal, or those residing in close proximity to the temporal bone. Magnetic susceptibility differences are more pronounced at the interface between two distinct biological entities (e.g., air-tissue). This is because local field variations lead to a more rapid dephasing of regional spins, resulting in geometric distortions, an overall loss of MRI signal, and a drop in BOLD sensitivity. The phase accumulation experienced by spins in high susceptibility regions manifests along the slice direction, thereby displacing the MR signal outside the encoding window. This can be partially overcome by the use of z-shim sequences, which have the potential to recover lost signal through the deployment of a z (slice select) gradient prior to acquisition. By altering spin coherence in this manner, it ensures that isochromats in these interface regions generate a complete in-phase echo. However, this has the undesirable effect of dephasing spins everywhere else. This necessitates a 2-shot approach by collecting both in-phase and out-of-phase information and reconstructing maximum intensity projections to arrive at a final result. One major drawback of this approach is that it effectively halves the temporal resolution of the acquired data and reduces hemodynamic response sampling and subsequent statistical power during analysis. To overcome this limitation, single-shot z-shim methods were developed to provide simultaneous spatial and temporal encoding (Fig. 20.10) where the classic EPI phase and slice gradient playouts are replaced by those detailed on the right [9]. The oscillating gradients along both the slice select and EPI phase encode directions allow for the acquisition of an image corresponding to the positive readout gradients and a second linked to the negative readouts. Each of these images is tied to a z-shim parameter that is derived through calibration scans built to optimize signal intensities across all slices. The oscillating nature of the slice select gradient during the EPI train controls the settings for both the positive and negative readout lines, allowing for rapid adjustment of the sampled slice during readout. While this method typically results in longer echo train, and thus an increase in geometric distortions, parallel imaging can be introduced to reduce these effects.

Arterial Spin Labeling

Arterial spin labeling (ASL) is another functional imaging technique that can be used to map neuronal activation in the brain. While BOLD fMRI assesses neuronal activity through changes in local blood oxygenation, ASL directly tracks perfusion through the quantification of cerebral blood flow (CBF) [10]. Simply stated, ASL uses the water in blood as an

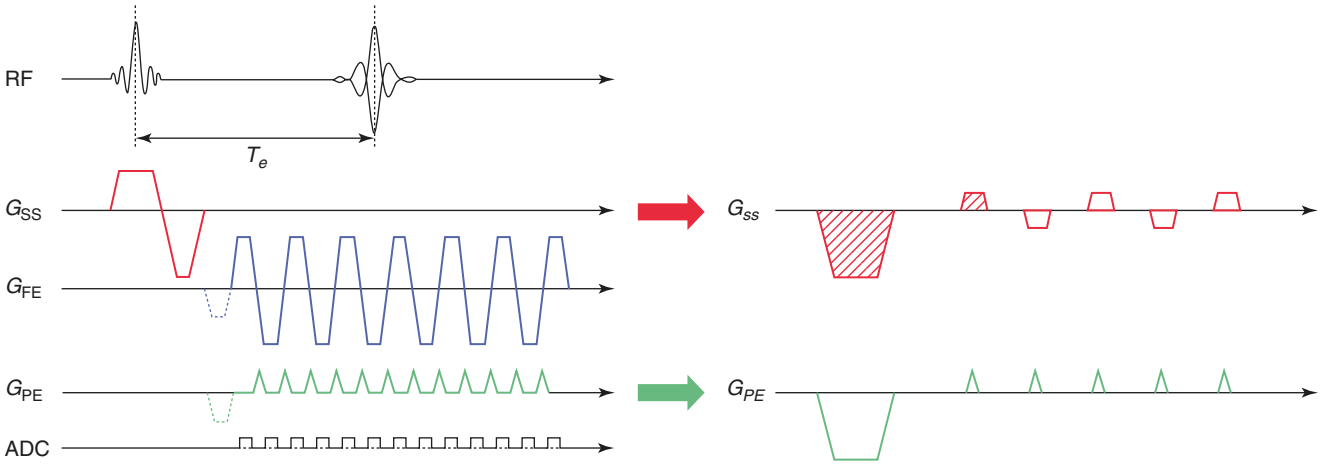

Fig. 20.10 Modification to the standard SS GRE EPI pulse sequence to incorporate z-shim correction

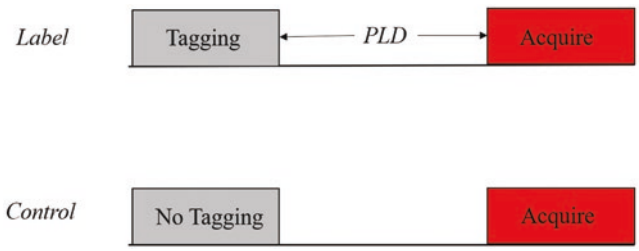

Fig. 20.11 Top-level schematic illustrating the difference between the label and control images needed for ASL quantification. The post label delay (PLD) represents the time allowed for tagged blood to travel into the brain

endogenous contrast agent via a labeling process and requires the acquisition of two distinct sets of images; those with and without an inversion pulse used to "tag" the spins in arterial blood prior to acquisition (shown in Fig. 20.11).

Once both the label and control datasets have been collected, they can be fit to a physiological model for CBF calculation, which is output on a voxel-wise basis in the clinically used measure of mL/100 g/min. At its core, ASL appears to be a relatively simple technique; however, several methods exist to prepare and manipulate the magnetic properties of inflowing arterial blood supply while balancing duration of labeled blood delivery versus decreased SNR (T1 decay) through parameter optimization. While continuous (CASL) and pulsed (PASL) ASL techniques exist independently, the current clinical recommendation is to use a pseudo-continuous (pCASL) labeling approach where spin tagging is achieved through rapid RF pulsing during the labeling period [11]. pCASL is an effective compromise between the CASL and PASL variants as it offers superior labeling efficiency while minimizing magnetization transfer effects leading to an overall higher SNR. This labeling scheme when used in conjunction with a gradient and spin echo (GRASE) readout is relatively insensitive to field inhomogeneities and thus provides superior SNR for ASL quantification [12, 13]. The GRASE sequence deploys a series of 180° refocusing pulses that when combined with a train of oscillating gradient readout lobes generate a collection of both gradient and spin echoes [14]. As the GRASE sequence is a hybrid of both the EPI and fast SE sequences, it overcomes some of the inherent limitations of each pulse sequence by offering a reduction in geometric distortions while lending itself to fast scan times and less energy deposition. ASL is arguably the most quantitative of all functional imaging techniques as it measures blood flow directly via labeling, rather than by inference from T2* dephasing as in BOLD, and has shown promise as a potential biomarker for early detection of Alzheimer's disease given the role of vascular dysregulation in current neuroscientific models for neurodegeneration [15].

Simultaneous Multislice (SMS) or Multiband Imaging

Becoming more ubiquitous in the advanced functional imaging space is multiband (MB), or simultaneous multislice (SMS), imaging. SMS is a technique that allows for tremendous acquisition acceleration by exciting multiple slices concurrently. This has a profound impact on scan time through substantial reductions in TR. From a functional imaging perspective, increasing temporal resolution enables dense sampling of the hemodynamic response providing a more comprehensive characterization when investigating neuronal correlates. SMS is achieved by summing RF waveforms with different phase modulations to achieve excitation at multiple slice locations. The composite pulse can now excite a unique band of frequencies that correspond to physical slices loca-

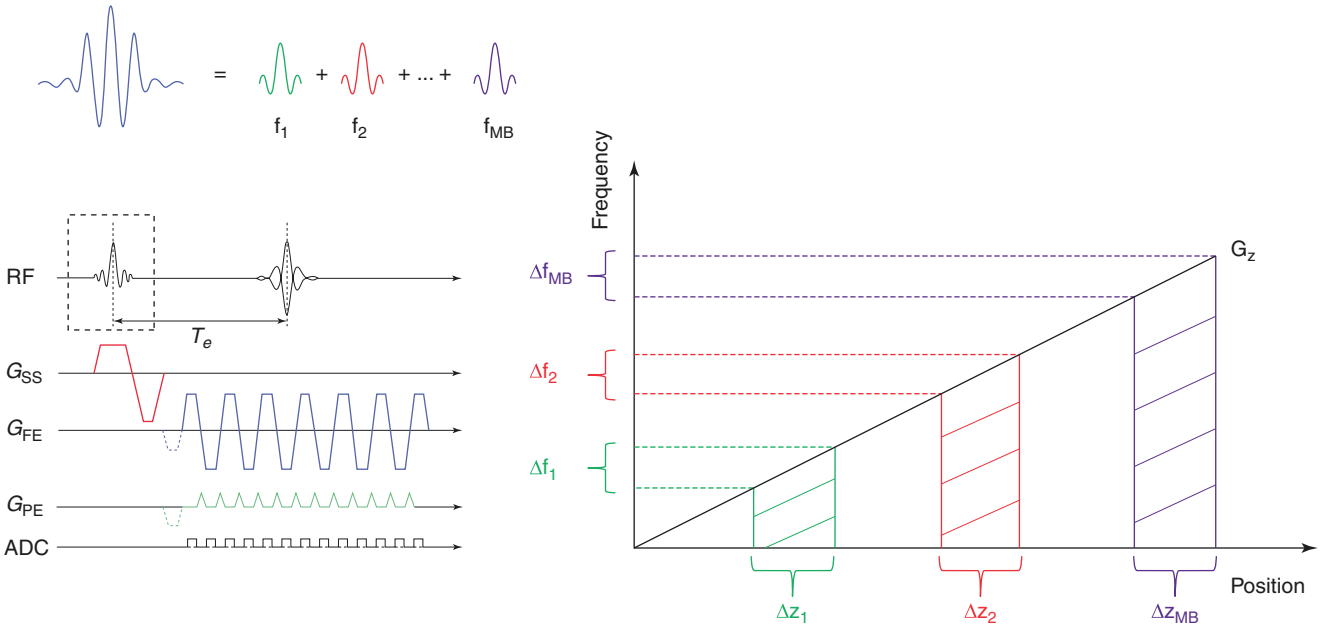

Fig. 20.12 SMS EPI excitation pulse and associated slice location profiles

tion relative to gradient isocenter (see Fig. 20.12). A standard GRE-EPI excitation can be replaced with the multiband pulse, where the MB factor (or number of unique RF waveforms) dictates the number of simultaneously acquired slices given a consistent and common slice select gradient.

However, despite the ability to simultaneously excite multiple slice locations, standard *k*-space encoding does not allow for the individual signals to be disentangled. To overcome this, coil encoding was introduced through development of SMS sampling and reconstruction methodologies. While many exist, the most common approach relies on forced, or controlled, aliasing along the phase encode direction. Images at the varying slices can then be parsed out based on coil sensitivity information, the details of which are beyond the scope of this analysis. SMS imaging has specific hardware requirements which may not be present on the majority of installed scanners. However, its availability is increasing as BOLD and diffusion EPI sequences become more widely used. Given the growing utilization of SMS imaging, it was important to mention. For additional technical details regarding the evolution and current standard of SMS imaging, please consult the following reference [16].

Multicontrast EPI (EPIMix)

Long acquisition times are one of the biggest drawbacks of MRI in clinical practice. This can have an adverse effect on patient compliance due to discomfort. This inevitable patient discomfort leads to an increased likelihood of motion-induced artifacts given the multishot nature of most clinical scans, particularly as total scan length increases. To account for this, many brain protocols are optimized to collect indication-specific contrasts early during the scan. However, in situations where a patient's condition is unknown, prioritizing scan order, which may alleviate patient burden, and ensuring the collection of images of sufficient quality can be challenging to balance. While motion/ghosting compensation can be achieved using techniques such as PROPELLER (**P**eriodically **R**otated **O**verlapping Parall**EL** **L**ines with **E**nhanced **R**econstruction) [17], the *k*-space oversampling tends to lead to prolonged scan times that could be counterproductive, particularly in trauma settings. In this context, recent research has focused on the use of single-shot EPI sequences for their speed and relative insensitivity to motion. This is extraordinarily novel as a routine trauma protocol typically consists of T1-weighted, T2-weighted, T2-fluid-attenuated inversion recovery (FLAIR), T2*, and diffusion-weighted imaging (DWI) acquisitions. Skare and colleagues have developed a modular abstraction layer integrated with pulse sequence programming framework [18]. Through this abstraction layer, different inversion, preparation, padding, and readout schemes can be combined together to allow for dynamic acquisition block capable of being collected within a single multicontrast sequence. This investigational approach requires more validation; however, early works have shown comparable lesion presentation relative to conventional scans [19].

Table 20.2 Key articles of scanning methods

Authors	Article title	Significance
Hahn [2]	Spin echoes	First demonstration of spin echo in NMR
Lauterbur [1]	Image formation by induced local interactions: Examples of employing nuclear magnetic resonance (NMR)	Introduction of the concept of spatial encoding
Mansfield [5]	Multi-planar imaging formation using NMR spin echoes	Development of echo planar imaging
Kwong et al. [7]	Dynamic magnetic resonance imaging of human brain activity during primary sensory stimulation	First human BOLD fMRI experiment
Williams et al. [10]	Magnetic resonance imaging of perfusion using spin inversion of arterial water	First paper to demonstrate arterial spin labeling

Conclusion

This chapter provided an overview of the physics behind the most prevalent sequences and methods used in fMRI (Table 20.2). Although a top-level perspective was provided, it is important to reemphasize that MRI is a technique of tradeoffs and that optimizing imaging parameters to maximize and enhance BOLD signal is paramount. The field of MRI is continuing to evolve as new, novel, and innovative acquisition and reconstruction schemes are developed. From routine clinical care to advanced imaging biomarker-driven therapeutics, validation is needed to transition these techniques from the research domain to clinical practice. As indication-specific neuroscientific models are proven and accepted, imaging needs to continue to adapt to aid in the identification and characterization of early pathophysiological change within the disease cascade.

References

1. Lauterbur P. Image formation by induced local interactions: examples employing nuclear magnetic resonance. Nature. 1973;242:190–1.
2. Hahn E. Spin echoes. Phys Rev. 1950;80:580–94.
3. Hahn E. Detection of sea-water motion by nuclear precession. J Geophys Res. 1960;65:776–7.
4. Ogawa S, Lee TM, Kay AR, Tank DW. Brain magnetic resonance imaging with contrast dependent on blood oxygenation. Proc Natl Acad Sci U S A. 1990;87:9868–72.
5. Mansfield P. Multi-planar imaging formation using NMR spin echoes. J Phys C Solid State Phys. 1977;10:L55–8.
6. Thulborn KR, Waterton JC, Matthews PM, Radda GK. Oxygenation dependence of the transverse relaxation time of water protons in whole blood at high field. Biochim Biophys Acta. 1982;714:265–70.
7. Kwong KK, Belliveau JW, Chesler DA, Goldberg IE, Weisskoff RM, Poncelet BP, et al. Dynamic magnetic resonance imaging of human brain activity during primary sensory stimulation. Proc Natl Acad Sci U S A. 1992;89:5675–9.
8. QIBA profile: mapping of sensorimotor brain regions using blood oxygenation level dependent (BOLD) functional MRI as a pre-treatment assessment tool. https://qibawiki.rsna.org/index.php/FMRI_Biomarker_Ctte.
9. Hoge SW, Pan H, Tan H, Stern E, Kraft RA. Efficient single-shot z-shim EPI via spatial and temporal encoding. In: IEEE ISBI; 2011. p. 1565–86.
10. Williams DS, Detre JA, Leigh JS, Koretsky AP. Magnetic resonance imaging of perfusion using spin inversion of arterial water. Proc Natl Acad Sci U S A. 1992;89(1):212–6.
11. Alsop D, et al. Recommended implementation of arterial spin-labeled perfusion MRI for clinical applications: a consensus of the ISMRM perfusion study group and the European consortium for ASL in dementia. Magn Reson Med. 2015;73:102–16.
12. Wu WC, Fernández-Seara M, Detre JA, Wehrli FW, Wang J. A theoretical and experimental investigation of the tagging efficiency of pseudocontinuous arterial spin labeling. Magn Reson Med. 2007;58:1020–7.
13. Fernández-Seara MA, Edlow BL, Hoang A, Wang J, Feinberg DA, Detre JA. Minimizing acquisition time of arterial spin labeling at 3T. Magn Reson Med. 2008;59:1467–71.
14. Feinberg D, Oshio K. GRASE (gradient-and spin-echo) MR imaging: a new fast clinical imaging technique. Radiology. 1991;181:597–602.
15. Iturria-Medina Y, Sotero RC, Toussaint PJ, Mateos-Pérez JM, Evans AC, Alzheimer's Disease Neuroimaging Initiative. Early role of vascular dysregulation on late-onset Alzheimer's disease based on multifactorial data-driven analysis. Nat Commun. 2016;7:11934.
16. Barth M, Breuer F, Koopmans PJ, Norris DG, Poser BA. Simultaneous multislice (SMS) imaging techniques. Magn Reson Med. 2016 Jan;75(1):63–81.
17. Pipe J. Motion correction with PROPELLER MRI: application to head motion and free-breathing cardiac imaging. Magn Reson Med. 1999;42(5):963–9.
18. Skare S, Sprenger T, Norbeck O, Rydén H, Blomberg L, Avventi E, et al. A 1-minute full brain MR exam using a multicontrast EPI sequence. Magn Reson Med. 2018;79:3045–54.
19. Delgado AF, Kits A, Bystam J, Kaijser M, Skorpil M, Sprenger T, et al. Diagnostic performance of a new multicontrast one-minute full brain exam (EPIMix) in neuroradiology: a prospective study. J Magn Reson Imaging. 2019;50:1824–33.